



The saturation state of the world's ocean with respect to (Ba,Sr)SO₄ solid solutions

Christophe Monnin, Damien Cividini

► To cite this version:

Christophe Monnin, Damien Cividini. The saturation state of the world's ocean with respect to (Ba,Sr)SO₄ solid solutions. *Geochimica et Cosmochimica Acta*, 2006, 70, pp.3290-3298. 10.1016/J.GCA.2006.04.002 . hal-00662992

HAL Id: hal-00662992

<https://hal.science/hal-00662992>

Submitted on 20 Feb 2013

HAL is a multi-disciplinary open access archive for the deposit and dissemination of scientific research documents, whether they are published or not. The documents may come from teaching and research institutions in France or abroad, or from public or private research centers.

L'archive ouverte pluridisciplinaire **HAL**, est destinée au dépôt et à la diffusion de documents scientifiques de niveau recherche, publiés ou non, émanant des établissements d'enseignement et de recherche français ou étrangers, des laboratoires publics ou privés.

The saturation state of the world's ocean with respect to (Ba,Sr)SO₄ solid solutions

Christophe Monnin^{*}, Damien Cividini¹

Laboratoire Mécanismes de Transfert en Géologie, CNRS/Université Paul Sabatier, 16 Avenue Edouard Belin, 31400 Toulouse, France

Received 7 December 2005; accepted in revised form 7 April 2006

Abstract

Barite is commonly found in suspended matter in ocean waters and in marine sediments. The calculation of the barite saturation index of the world's ocean waters has shown that the vast majority of the oceans are undersaturated with respect to pure barium sulfate, equilibrium being reached at a few locations like the Southern Ocean surface waters, deep waters of the Bay of Bengal or intermediate waters of the Pacific [Monnin, C., Jeandel, C., Cattaldo, T., Dehairs, F. 1999. The marine barite saturation state of the world's oceans. *Mar. Chem.* **65** (3–4), 253–261.]. It is thus paradoxical to commonly find barite in a globally undersaturated ocean. Strontium is the most common impurity in natural barite. It is often suggested that the Ba content of ocean waters is controlled by equilibrium with Sr-substituted barite, and not with pure BaSO₄. In order to address this problem, we have used the GEOSECS data (49 stations, 1404 data points) to calculate the saturation index of substituted barite in the world's ocean using Lippmann's description of thermodynamic equilibrium between a solid solution and an aqueous solution for the (Ba,Sr)SO₄ system. Recent studies indicate that the (Ba,Sr)SO₄ solid solution is most likely regular and continuous. The calculated saturation indices of the regular solid solution (with the interaction parameter A_0 equal to 1.6) are closer to those of pure barite than those calculated for the ideal solid solution. Conclusions previously reached for the pure barite case are not changed: the saturation state of ocean waters with respect to a regular solid solution is very close to that of pure barite. Sr-substitution for Ba in barium sulfate does not bring barite at equilibrium. When equilibrium is reached, the degree of Sr substitution of Ba amounts to only a few mole percent of Sr. Equilibrium values of the Sr content of the solid solutions in the intermediate (0.2–0.8) range are found for ocean surface waters where the Ba/Sr ratio is low, but as these waters are undersaturated, such solids are not stable in the water column. This provides another reason for the bimodal distribution of (Ba,Sr)SO₄ solid solutions in nature, on top of that induced by the large ratio of the end member solubility products. Equilibrium is found for cold waters (i.e. for temperatures below 5 °C) having a Ba content greater than about 70 nmol/kg. The distribution coefficient of Sr in barite can be calculated from the Ba and Sr concentrations of these samples and from the equilibrium Sr mole fraction of the solid solution obtained from Lippmann's diagram. It was found independent of pressure and it varies only slightly with the temperature of the sample. For the regular solid solution (with $A_0 = 1.6$), it is:

$$10^5 D_{\text{BaSO}_4}^{\text{Ba}}(\text{regular}) = 10^5 \left[\frac{m_{\text{Ba}^{2+},\text{aq}}}{m_{\text{Sr}^{2+},\text{aq}}} \frac{x_{\text{BaSO}_4,\text{SS}}}{x_{\text{SrSO}_4,\text{SS}}} \right] = 0.227t + 3.753.$$

This expression (which has been established for temperatures below 5 °C) can be used to directly calculate the composition of solid solutions at equilibrium with a given seawater sample, or conversely to know the Ba content of seawater at equilibrium with a given (Ba,Sr)-SO₄ solid solution.

© 2006 Published by Elsevier Inc.

1. Introduction

In the ocean, the correlation between dissolved barium and biointermediate elements like alkalinity and silica

^{*} Corresponding author.

E-mail address: monnin@lmtg.obs-mip.fr (C. Monnin).

¹ Present address: Centre de Géochimie de la Surface, CNRS/Université Louis Pasteur, 1 rue Blessig, 67084 Strasbourg, France.

(Chan et al., 1977; Jeandel et al., 1996), and the fact that Ba can be preserved as refractory barite in the sedimentary record have generated numerous studies for the use of this element as a proxy in paleoceanography. The presence of barite is commonly reported in suspension in the water column (Jacquet et al., 2004; Sternberg et al., 2005) and in sediments (Van Beek et al., 2003). On the other hand, thermodynamic calculations have established that the world ocean is globally undersaturated (Monnin et al., 1999; Rushdi et al., 2000). This paradox underlines the question of the mode of formation of marine barite and their stability in the marine environment.

There is an obvious role of living organisms in barite formation (see the discussion in Sternberg et al., 2005), some living organisms being able to directly form barite within their cells (Gooday and Nott, 1982). It is also commonly accepted that barite saturation can be reached in microenvironments of decaying organic matter (Dehairs et al., 1987). On the other hand, Acantharia build their skeleton with strontium sulfate (celestine), which incorporates as much as 10 mol% of barium (Bernstein et al., 1992). Celestine formation by Acantharia is a case of mineral formation in a thermodynamically unfavorable pathway. When these organisms die, their skeletons dissolve in the surrounding water (which is largely undersaturated with respect to celestine), and barium is then released to the aqueous phase. This leads to a local enrichment of barium and therefore to the inorganic formation of barite, that may in turn incorporate some strontium (Bernstein et al., 1992).

This latter mode of formation of marine barite directly addresses the influence of impurities on barite stability. It can be shown that a solution at equilibrium with a solid solution is always undersaturated with respect to the pure end members, although this undersaturation may be very slight when the difference between the endmember solubility products is large (Glynn and Reardon, 1990). It can then be postulated that the world ocean, which is globally undersaturated with respect to pure BaSO₄ (Monnin et al., 1999), may in fact be at equilibrium with Sr-substituted barite. This would provide an explanation of the barite paradox.

The geological/oceanographic problem is that of the stability of barite in the marine environment. Modeling first translates this problem into the calculation of the solubility (or equivalently the saturation index) of a solid phase used as a model for natural barite in a model system for seawater. Marine barites (the natural products, with their impurities, crystal defects, poor crystallinity, etc.) have been represented so far by pure solid barium sulfate (Monnin et al., 1999; Rushdi et al., 2000), although the question of Sr-substitution in marine barite has often been addressed (see below). Thermodynamic models for seawater are numerous. They can differ by the number of species they take into account, by the methods used to calculate the thermodynamic properties of the dissolved species and by the temperature, pressure

and concentration ranges they can account for. A lot of effort has been made to improve our ability to calculate the thermodynamic properties of electrolyte solutions in general, and natural waters like seawater in particular. Among many others, Monnin (1999) has elaborated a model based on Pitzer's ion interaction approach to calculate the solubilities of barite and celestine in the Na–K–Ca–Mg–Ba–Sr–Cl–SO₄–H₂O system as a function of solution composition, temperature and pressure. This model has been used by Monnin et al. (1999) to address the problem of barite stability in seawater by calculating the saturation state of barite in the world ocean using mainly the GEOSECS data base. It could be objected that the Na–K–Ca–Mg–Ba–Sr–Cl–SO₄–H₂O system does not take into account dissolved species or compounds (like carbonate or bicarbonate, low molecular weight organic acids, colloids, etc.; Putnis et al., 1995) that may build complexes with aqueous barium in seawater, therefore changing its thermodynamic properties. Strong complexing generally lowers the total activity coefficients of dissolved electrolytes. This would lead to a decrease in the barite saturation index, thus worsening the barite paradox. The extension of the description of the aqueous phase at the level of accuracy reached by models based on Pitzer's ion interaction approach should be given some attention, despite the large research effort it requires.

The influence of strontium substitution on barite stability in the marine environment has been addressed in early papers on this topic (Hanor, 1969; Church and Wolgemuth, 1972). We here take advantage of recent progress in the study of aqueous solution–solid solution systems (Glynn and Reardon, 1990; Konigsberger and Gamsjager, 1992; Prieto et al., 1993; Prieto et al., 1997; Glynn, 2000; Astilleros et al., 2003). The present work presents the calculation, based on Lippmann diagrams, of the saturation state of the world's ocean with respect to, and the composition of, Sr-substituted barite at equilibrium with seawater. These calculations have been carried out for the 1404 seawater samples collected at the 49 GEOSECS stations for which the Ba content is reported (Ostlund et al., 1987), which provides a view of the global ocean.

2. Depicting thermodynamic equilibrium in the Lippmann diagram

By analogy with classical temperature–composition phase diagrams, Lippmann (Lippmann, 1980, 1982) has constructed a diagram that allows the calculation of the composition of solid solutions at equilibrium with aqueous solutions. We write here the various expressions for the case of a (Ba,Sr)SO₄ solid solution. The general theory can be found in Glynn (2000); Glynn and Reardon (1990) and Lippmann (1977, 1980, 1982). The conditions for thermodynamic equilibrium can be expressed as:

$$K_{\text{BaSO}_4} = \frac{a_{\text{Ba}^{2+},\text{aq}} \cdot a_{\text{SO}_4^{2-},\text{aq}}}{x_{\text{BaSO}_4,\text{ss}} \cdot f_{\text{BaSO}_4,\text{ss}}} \quad (1)$$

and

$$K_{\text{SrSO}_4} = \frac{a_{\text{Sr}^{2+},\text{aq}} \cdot a_{\text{SO}_4^{2-},\text{aq}}}{x_{\text{SrSO}_4,\text{ss}} \cdot f_{\text{SrSO}_4,\text{ss}}} \quad (2)$$

In Eqs. (1) and (2) K_{BaSO_4} and K_{SrSO_4} are the solubility products of the solid solution end members, x their mole fraction and f their activity coefficient in the solid solution. a is the activity of the designated aqueous species. Lippmann (1980, 1982) defined the total ionic product $\Sigma\Pi$:

$$\Sigma\Pi = a_{\text{SO}_4^{2-},\text{aq}} \cdot (a_{\text{Ba}^{2+},\text{aq}} + a_{\text{Sr}^{2+},\text{aq}}) \quad (3)$$

Eqs. (1) and (2) can be substituted in Eq. (3) to derive the expression of the total ionic product at thermodynamic equilibrium $\Sigma\Pi_{\text{eq}}$. This leads to the expression of the solidus:

$$\Sigma\Pi_{\text{eq}} = x_{\text{BaSO}_4,\text{ss}} \cdot f_{\text{BaSO}_4,\text{ss}} \cdot K_{\text{BaSO}_4} + x_{\text{SrSO}_4,\text{ss}} \cdot f_{\text{SrSO}_4,\text{ss}} \cdot K_{\text{SrSO}_4} \quad (4)$$

Lippmann introduced the ionic activity fractions of the dissolved species:

$$\chi_{\text{Ba}^{2+}} = \frac{a_{\text{Ba}^{2+}}}{a_{\text{Ba}^{2+}} + a_{\text{Sr}^{2+}}} \quad (5)$$

and

$$\chi_{\text{Sr}^{2+}} = \frac{a_{\text{Sr}^{2+}}}{a_{\text{Ba}^{2+}} + a_{\text{Sr}^{2+}}} \quad (6)$$

These quantities are used in another relationship called the *solutus* that allows expressing the total ionic product at equilibrium as a function of the aqueous solution composition:

$$\Sigma\Pi_{\text{eq}} = \frac{1}{\frac{\chi_{\text{Ba}^{2+},\text{aq}}}{K_{\text{BaSO}_4} \cdot f_{\text{BaSO}_4,\text{ss}}} + \frac{\chi_{\text{Sr}^{2+},\text{aq}}}{K_{\text{SrSO}_4} \cdot f_{\text{SrSO}_4,\text{ss}}}} \quad (7)$$

So equilibrium can be depicted by plotting Eqs. (4) and (7) in a diagram with $\Sigma\Pi$ in the vertical axis and two superimposed horizontal axes: the solid phase mole fraction for one and the ionic activity fraction for the other. Such a diagram can be used to estimate the composition of a solid solution at equilibrium with an aqueous solution of known composition, or conversely to know the composition of the aqueous phase at equilibrium with a solid solution of a given composition. We refer here to thermodynamic (or true) equilibrium for which Eqs. (1) and (2) are fulfilled. We do not consider partial equilibrium states in solid solution–aqueous solution systems like stoichiometric saturation and primary saturation states that are very useful in reaction path analysis of dissolution and precipitation of solid solutions (Glynn and Reardon, 1990; Königsberger and Gamsjager, 1992; Prieto et al., 1993; Prieto et al., 1997; Glynn, 2000).

Lippmann diagrams can be used to depict the saturation state of a given aqueous solution with respect to a solid

solution of varying composition. For this one can define $\Omega(x)$, the saturation index of the aqueous solution as:

$$\Omega(x) = \frac{\Sigma\Pi}{\Sigma\Pi_{\text{eq}}(x)} \quad (8)$$

$\Sigma\Pi$ is the total ionic product Eq. (3) and $\Sigma\Pi_{\text{eq}}(x)$ is the total ionic product for an aqueous solution with the same ionic activity fraction than the aqueous solution under consideration, at thermodynamic equilibrium with a solid solution of mole fraction x , the value of which is calculated using Lippmann's diagram, as detailed below. The calculation of the saturation index is a case of reverse modeling, in which one starts from the aqueous solution composition to infer the equilibrium state of the solid solution–aqueous solution (SSAS) system, by contrast with forward modeling in which one would calculate the solid solubility and compare it with the observed composition of the solution (Plummer, 1992).

Multiplying the top and bottom of Eqs. (5) and (6) by the activity coefficient of dissolved sulfate, the barium activity fraction can be written as:

$$\chi_{\text{Ba}^{2+}} = \frac{1}{1 + \frac{m_{\text{Sr}^{2+},\text{aq}}}{m_{\text{Ba}^{2+},\text{aq}}} \cdot \left(\frac{\gamma_{\text{SrSO}_4,\text{aq}}}{\gamma_{\text{BaSO}_4,\text{aq}}} \right)^2} \quad (9)$$

(with a similar expression for Sr). In Eq. (9), m is the molality of the designated species. When given by the chemical analysis, it is the total concentration of this aqueous element. In this case, the γ are the total (or stoichiometric) activity coefficients of the designated aqueous electrolyte, namely $\text{BaSO}_{4,\text{aq}}$ and $\text{SrSO}_{4,\text{aq}}$. They can be calculated by any aqueous solution model. In this work, we have used the barite and celestine solubility model of Monnin (1999). Based on Pitzer's ion interaction approach, it allows the calculation of the thermodynamic properties of aqueous electrolytes in a wide range of solution concentration and composition in the Na–K–Ca–Mg–Ba–Sr–Cl– SO_4 – H_2O system, from infinite dilution to brines, from 0 to 200 °C and from 1 bar to 1 kbar. Monnin (1999) also give the barite and celestine solubility products K_{BaSO_4} and K_{SrSO_4} that are needed in Eqs. (4) and (7).

Given the aqueous solution composition, the total ionic product can be calculated as:

$$\Sigma\Pi = m_{\text{SO}_4^{2-},\text{aq}} \cdot \left(m_{\text{Ba}^{2+},\text{aq}} \cdot \gamma_{\text{BaSO}_4,\text{aq}}^2 + m_{\text{Sr}^{2+},\text{aq}} \cdot \gamma_{\text{SrSO}_4,\text{aq}}^2 \right) \quad (10)$$

So the i th aqueous solution can be represented in a Lippmann diagram by its barium activity fraction $\chi_{\text{Ba}^{2+},\text{aq}}(i)$ and its total ionic product $\Sigma\Pi_i$ (Fig. 1).

In order to calculate the saturation index Ω , we need to calculate the total ionic product at equilibrium $\Sigma\Pi_{\text{eq}}$. This requires knowing the thermodynamic properties of the solid solution, i.e. the activity coefficients of its components (see next section). $\Sigma\Pi_{\text{eq}}$ is calculated by iteration as follows. Starting from an initial guess of the barium mole fraction in the solid solution, $x_{\text{BaSO}_4,\text{ss}}$, Eq. (4) is used to calculate $\Sigma\Pi_{\text{eq}}$. Eq. (7) is solved for the aqueous barium activity fraction,

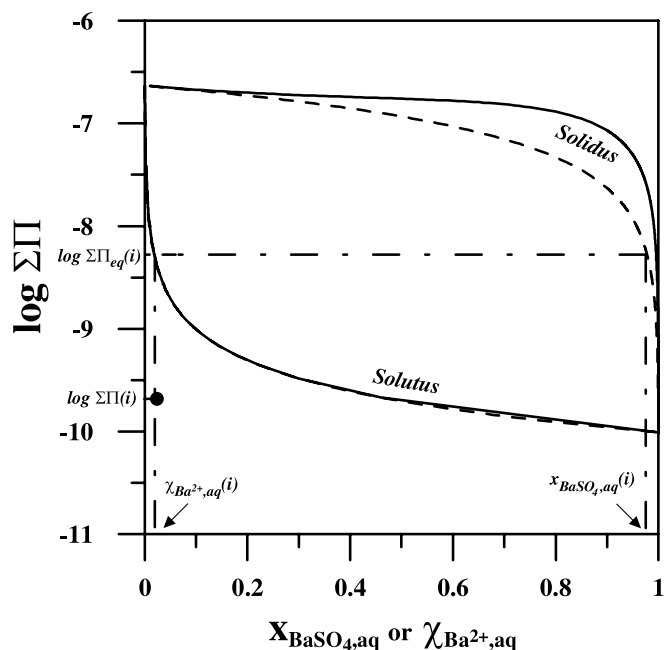


Fig. 1. Lippmann diagram for the ideal (Ba,Sr)SO₄ solid solution. The dashed curves are those for the case of the ideal solution and the plain ones for a regular solid solution (with $A_0 = 1.6$). The black dot represents an aqueous solution whose equilibrium state can be inferred from such a diagram (undersaturation in this case). $\Sigma\Pi$ is the total ionic product of the considered aqueous solution of barium ionic activity fraction $\chi_{\text{Ba}^{2+},\text{aq}}$. $\Sigma\Pi_{\text{eq}}(x)$ is the total ionic product for an aqueous solution with the same ionic activity fraction than the aqueous solution under consideration, at thermodynamic equilibrium with a solid solution of barium mole fraction $x_{\text{BaSO}_4,\text{ss}}$.

$\chi_{\text{Ba}^{2+},\text{aq}}$. Then $x_{\text{BaSO}_4,\text{ss}}$ is incremented until $\chi_{\text{Ba}^{2+},\text{aq}}$ is equal (within the ascribed numerical allowance) to its value for the aqueous solution under consideration. The last value of $x_{\text{BaSO}_4,\text{ss}}$ is then the equilibrium composition of the solid solution in contact with this aqueous phase.

Fig. 1 illustrates the case of an undersaturated solution in a Lippmann diagram drawn for two cases of (Ba,Sr)SO₄ solid solutions: the ideal solution (dashed curves) and the regular solid solution (plain curves; see below). As already noted in several instances (Glynn and Reardon, 1990; Glynn et al., 1992; Prieto et al., 1993; Prieto et al., 1997), the solutus of the Lippmann diagram for (Ba,Sr)SO₄ decreases very rapidly at small barium activity fractions, then levels off. A symmetrical behavior is observed for the solidus: its variation is small over an extended range of barium activity fraction, before it decreases very rapidly at high barium activity fractions. This shape of the Lippmann diagram is due to the large ratio between the barite and celestine solubility products: at 25 °C, $\text{Log}K_{\text{sp}} = -10.05$ for barite and $\text{Log}K_{\text{sp}} = -6.63$ for celestine (Monnin, 1999). This results in large fractionations between barium and strontium at equilibrium: an aqueous solution with very small barium to strontium ratio will be at equilibrium with an almost pure barite (or with a weakly substituted barium sulfate phase). This has been proposed as an explanation of the bimodal distribution of the

composition of natural barite and celestine in nature, and of the very rare occurrence of solid solutions of intermediate compositions (Prieto et al., 1993, 1997; Hanor, 2000).

Also depicted in Fig. 1 is the difference between the ideal and regular solutions (see below). The solutus of the ideal and regular solutions are almost indistinguishable, while the solidus of the regular solution has a more pronounced curvature than that of the ideal solution.

3. Thermodynamic properties of the (Ba,Sr)SO₄ solid solution

Despite numerous studies, the thermodynamic properties of the (Ba,Sr)SO₄ solid solution are still not firmly established (Hanor, 2000; Becker et al., 2000; Zhu, 2004). Experimentally this uncertainty comes from the methods of observations (Hanor, 2000). When using high temperature data like synthesis under hydrothermal conditions (e.g. Kotelnikov et al., 2000), there is a real difficulty in extrapolating the data back to low temperatures. In turn observations at low temperature were based on reaction path analysis of dissolution and precipitation experiments (e.g. Galinier et al., 1989; Felmy et al., 1993). In this case sluggish kinetics and compositional zoning in precipitating crystals are two likely reasons why true equilibrium may not be reached.

The existence of a miscibility gap is still under debate. Becker et al. (2000) reviewed the situation and concluded from their calculations from first principles, that the solid solution is not ideal. In a related paper, Prieto et al. (2000) represented the free energy of mixing of the solid solution with a Guggenheim expansion series up to the fourth order, leading to a non-regular symmetric solid solution with a very large miscibility gap (from 2.1 to 97.9 mol% SrSO₄). The simplest model for the representation of the thermodynamic properties of solid solutions is the regular solution model. In this model, the activity coefficient of the first component is a quadratic function of the mole fraction of the other component (e.g. Pitzer and Brewer, 1961; Guggenheim, 1967; Prigogine and Kondepudi, 1999). For the (Ba,Sr)SO₄ system, it leads to:

$$\ln f_{\text{BaSO}_4,\text{ss}} = \frac{w}{RT} \times x_{\text{SrSO}_4,\text{ss}}^2 \quad (11)$$

and, similarly

$$\ln f_{\text{SrSO}_4,\text{ss}} = \frac{w}{RT} \times x_{\text{BaSO}_4,\text{ss}}^2 \quad (12)$$

One also commonly finds the notation $A_0 = w/RT$. There exists a critical mixing temperature for regular solutions: the system presents a miscibility gap for A_0 values greater than 2 (Guggenheim, 1967; Prigogine and Kondepudi, 1999). In his compilation of the thermodynamic properties of halide, sulfate and carbonate solid solutions, Glynn (2000) reported various A_0 values leading to a large disagreement between authors about the existence of a miscibility gap. Finally Glynn (2000) retained an A_0 value of 2 to construct Lippmann's diagram. Zhu (2004) has

obtained a value of 1.53 for A_0 from a theoretical evaluation of the thermodynamic properties of binary solid solutions in the barite isostructural family. This is close to the value estimated by Galinier et al. (1989) who give $A_0 = 1.6$. These data (Galini er et al., 1989; Zhu, 2004) imply that the (Ba,Sr)SO₄ solid solution is regular and complete (continuous). In what follows we have carried out calculations for the ideal solution and for the regular solution model with the A_0 value of Galini er et al. (1989), for want of a definitive model for the (Ba,Sr)SO₄ solid solution.

4. The saturation state of the world ocean with respect to (Ba,Sr)SO₄ solid solutions

Monnin et al. (1999) have calculated the pure barite saturation index of ocean waters mainly from GEOSECS data (Ostlund et al., 1987) using the barite solubility model of Monnin (1999). The barium content is reported in the GEOSECS publications (Ostlund et al., 1987) for 49 stations, which amounts to 1404 data points. The original data (barium content in mol/kg seawater, salinity, temperature depth) has been converted to temperature, pressure and solution composition in molality by Monnin et al. (1999). These authors also give the list and the location of GEOSECS stations used in their paper that we also use in the present work.

Monnin et al. (1999) have found that the world ocean is mostly undersaturated with respect to pure BaSO₄. Equilibrium is reached in a few but notable places: surface waters of the Southern Ocean, intermediate waters (between 2000 and 3500 m) of the Pacific, deep waters (below 2000 m) of the Gulf of Bengal. These results were con-

firmed by Rushdi et al. (2000) with the use of a different thermodynamic model.

In this work, we have found that equilibrium (indicated by a saturation index between 0.9 and 1.1) is reached for 229 samples, 114 solutions are supersaturated and 1056 undersaturated. Equilibrium (or supersaturation) is achieved when the waters are cold (temperature below 5  C) and the Ba content greater than about 70 nmol/kg.

We focus on three examples of GEOSECS stations where equilibrium is reached. Fig. 2 displays the results for GEOSECS Station 445 (Bay of Bengal). This station is one of the cases where equilibrium is reached. The saturation indices of pure barite, of the ideal solid solution and of the regular solid solution are depicted versus depth (in meters below sea level, or mbsl) in Fig. 2. The pure barite saturation index and that of the regular solid solution are very close while the value for the ideal solid solution is offset by about 0.1. This example first shows that the saturation state of the world ocean is not drastically changed by the fact that strontium substitution in barite is taken into account, whatever model is used for the thermodynamic properties of the solid solution, contrarily to what one would have expected. As such, the conclusions about the saturation state of the world ocean with respect to barite (Monnin et al., 1999) do not change. It is not necessary to assume, as Rushdi et al. (2000) did, that Sr substitution in marine barite modify the saturation state of the ocean by 30%. Fig. 2 also displays the equilibrium value of the barium mole fraction of the solid solution. It can be seen that when the aqueous phase is saturated with respect to barite (i.e. for depths below about 1500 mbsl for the case of GEOSECS station 445), the barium mole fraction is roughly constant, at values between about 0.8 and 0.9 for the ideal

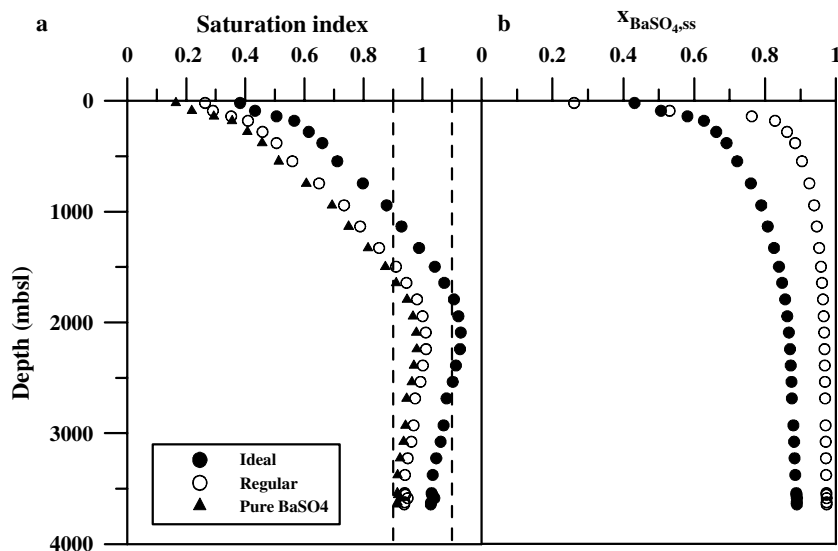


Fig. 2. GEOSECS Station 445 (Gulf of Bengal). (a) Variation with depth of the saturation index of pure barite (black triangles), of the ideal (Ba,Sr)SO₄ solid solution (black dots) and of the regular solid solution with $A_0 = 1.6$ (open dots). The dashed lines delimit the saturation index range within which equilibrium is assumed (i.e. between 0.9 and 1.1). (b) The equilibrium barium mole fraction of the solid solution versus depth.

solid solution, and between 0.95 to 0.98 for the regular solid solution.

Fig. 3 displays the results for GEOSECS Station 287 (Pacific sector of the Southern Ocean). This is the only case of the whole GEOSECS data set that exhibits a slight supersaturation for the surface waters, then a decreasing trend of the saturation index with depth until undersaturation is reached below about 2000 mbsl. In this case, the calculated barium mole fraction of the solid solution at equilibrium is constant at values of about 0.85 for the ideal solid solution and of about 0.96 for the regular one.

Station 263 (Central equatorial Pacific; Fig. 4) presents an example of the case (representative of the Pacific Ocean) where saturation is reached for waters at intermediate depths (between 1000 and 3000 mbsl). We find the same values of $x_{\text{BaSO}_4, \text{ss}}$ as for Station 445.

Barium in ocean waters is depleted in surface waters and regenerated at depth, to use the oceanographic parlance (Chan et al., 1977; Jeandel et al., 1996). Figs. 2 and 4 show that, when the barium to strontium ratio of the aqueous phase (or equivalently the barium activity fraction) is low (i.e. at the top of the water column), solid solutions of intermediate compositions (barium mole fraction between 0.2 and 0.8) are the stable phases. But because these waters with low Ba content are undersaturated with respect to these solid solutions, they cannot form through an inorganic process. If any biological process leads to the formation of such phases, they should dissolve when put in the conditions of open ocean waters. So, this undersaturation of ocean waters with respect to solid solutions of intermediate compositions provides another reason for the rare occurrence of such

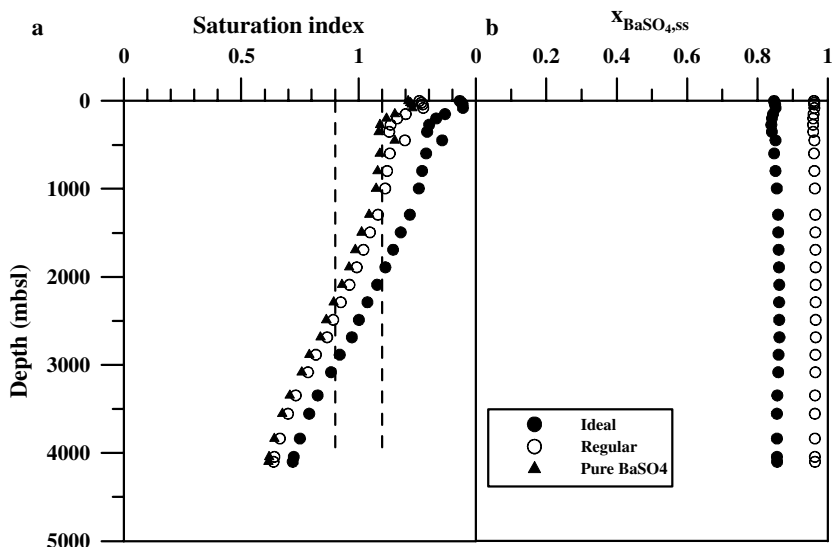


Fig. 3. GEOSECS Station 287 (Southern Ocean). See caption of Fig. 2.

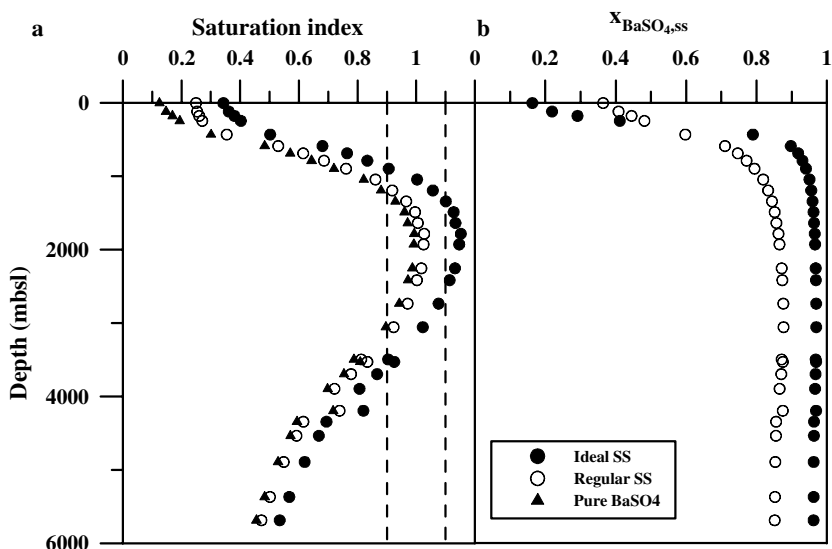


Fig. 4. GEOSECS Station 263 (Central equatorial Pacific). See caption of Fig. 2.

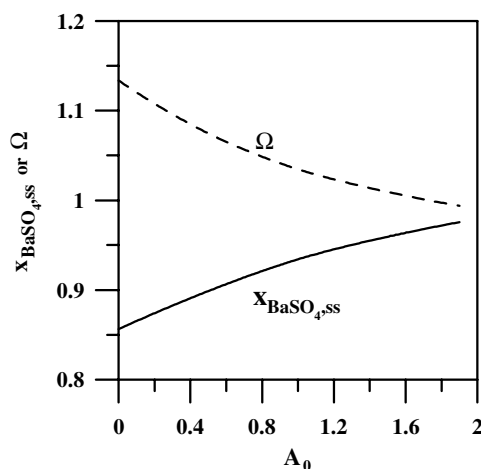


Fig. 5. The equilibrium mole fraction of barium in the solid solution and the saturation index Ω (Eq. (8) in the text) of the aqueous solution as a function of the A_0 parameter of the regular solid solution for the water sample at 1637 mbsl at Geosecs Station 263. Note that this sample is at equilibrium with a regular solid solution ($A_0 = 1.6$; see text) having a barium mole fraction of 0.97.

minerals (Tekin et al., 2002), in addition to the strong Ba/Sr fractionation induced by the large celestine to barite solubility product ratio (see Section 2).

We have calculated the variation of the saturation index and of the barium content of the solid solution, with the A_0 parameter of the solid solution. We took the example of the sample collected at 1637 mbsl at Geosecs Station 263 (Central equatorial Pacific) for which equilibrium is found (Fig. 5). $x_{\text{BaSO}_4, \text{ss}}$ increases with A_0 , from 0.85 for the ideal solution to 0.97 for the solid solution with $A_0 = 2$. The solid solution saturation index decreases toward the value for pure BaSO_4 (0.97 in this case). This is the consequence of the fact that the solidus of the regular solution lies above that for the ideal solution (Fig. 1). It thus appears that, even if future studies show that the non-ideality of the (Ba,Sr) SO_4 solid solution is larger than that of the simple regular model, effects of the non-ideality of the solid solution cannot correct its saturation index in the world ocean to bring it to the equilibrium value, as one would have expected in order to solve the paradox of the ubiquitous presence of barite in the marine environment.

5. Distribution coefficients and the Sr content of marine barite

Averyt and Paytan (2003) and Van Beek et al. (2003) have measured the composition of marine barite from sediment cores. They report values of the Sr over Ba concentration ratio in a range from 0.025 to 0.050 mol/mol. Averyt and Paytan (2003) also report small amounts of Ca in barite. These data translate into a Sr content in barite, of 2–4 mol%. This is in agreement with what we find here for the regular solution, and also with what has always been commonly admitted since the pioneering work of Church and Wolgemuth (1972). In

turn, Rushdi et al. (2000) have concluded, from what they report as approximate calculations, that marine barite may contain up to 13 mol Sr %. These authors have used an ideal solid solution model. Their result is consistent with ours: the Sr substitution at equilibrium is larger for the ideal solid solution than for the regular one (see above).

Distribution coefficients (also called partition coefficients) are empirical measures of the composition of a solid solution at equilibrium with an aqueous solution (see Glynn and Reardon (1990) for an outline of the development and use of distribution coefficients in SSAS systems). They often provide the experimental quantities from which one may try to extract thermodynamic constants. Hanor (2000) has reviewed the literature data for the case of natural and synthetic barite. As for the thermodynamic properties of the (Ba,Sr) SO_4 solid solution, the scatter in the data prevents any value to be recommended. To add to the confusion, distribution coefficients can be defined in several ways. The simplest definition is the ratio of two ratios: that of concentrations (in the molality scale) in the aqueous phase, to that of concentrations (in the mole fraction scale) in the solid solution:

$$D_{\text{BaSO}_4}^{\text{Ba}} = \frac{\frac{m_{\text{Ba}^{2+}, \text{aq}}}{m_{\text{Sr}^{2+}, \text{aq}}}}{\frac{x_{\text{BaSO}_4, \text{ss}}}{x_{\text{SrSO}_4, \text{ss}}}} = \frac{\frac{m_{\text{Ba}^{2+}, \text{aq}}}{m_{\text{Sr}^{2+}, \text{aq}}}}{\frac{x_{\text{BaSO}_4, \text{ss}}}{1 - x_{\text{BaSO}_4, \text{ss}}}} \quad (13)$$

$D_{\text{BaSO}_4}^{\text{Ba}}$ is then an apparent equilibrium constant and as such depends not only on temperature and pressure, but also on solution composition. An alternate definition (Glynn and Reardon, 1990) uses activities of dissolved species in the numerator of Eq. (13), while retaining mole fractions in the denominator. When activities are used instead of mole fractions and molalities in (13), then $D_{\text{BaSO}_4}^{\text{Ba}}$ is an equilibrium constant sometimes called the thermodynamic partition coefficient (e.g. Hanor, 2000).

When defined as in Eq. (13), distribution coefficients provide a direct and simple way to calculate the composition of the solid solution at equilibrium with a given aqueous solution without having to calculate the thermodynamic of the aqueous phase. In this work, we have calculated the distribution coefficients as defined by Eq. (13) from the values of the barium mole fraction of the solid solution and from the barium and strontium contents of the GEOSECS samples that were found at equilibrium, i.e. those for which the saturation index Eq. (8) is between 0.9 and 1.1. As noted above equilibrium is reached for cold waters. The distribution coefficients can only be calculated for narrow temperature ranges, of a few degrees above 0 °C (Fig. 6). The $D_{\text{BaSO}_4}^{\text{Ba}}$ values generated this way do not exhibit any trend with pressure or with the Ba content of the solution, but they show a slight increase with temperature (Fig. 6). They can be represented by the following expressions (in which T is the temperature in Celsius degrees):

$$10^5 D_{\text{BaSO}_4}^{\text{Ba}} (\text{ideal}) = 0.797T + 17.06 \quad (14)$$

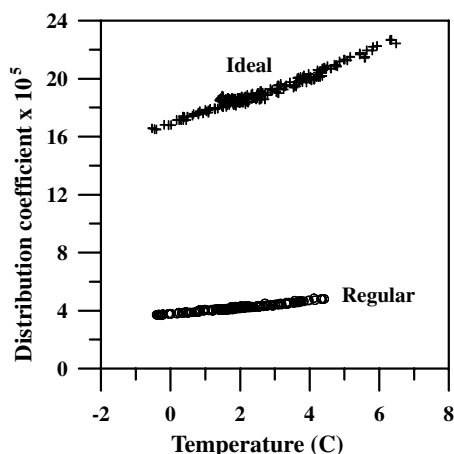


Fig. 6. Variation of the Ba distribution coefficient in (Ba,Sr)SO₄ with temperature for the ideal and regular solid solutions, calculated from the composition of the GEOSECS seawater samples for which equilibrium was found.

and

$$10^5 D_{\text{BaSO}_4}^{\text{Ba}}(\text{regular}) = 0.227T + 3.753 \quad (15)$$

The distribution coefficient for the ideal solution is 4–5 times larger than the one for the regular solid solution. This means that for a given ratio of the Ba to Sr content of the aqueous phase, the equilibrium composition of the ideal solid solution will be 4–5 times larger than that of the regular solution. This is another way of expressing the results depicted in Figs. 2–4: when the equilibrium Sr content of barite is about 3% for the regular solid solution, it is about 12–15% for the ideal solid solution.

We find a mean value of $D_{\text{BaSO}_4}^{\text{Ba}}(\text{regular})$ of about 4.2×10^{-5} . Averyt and Paytan (2003) report a distribution coefficient of 2.9×10^{-5} . This agreement may be fortuitous due to the uncertainty about what this value refers to due to the ambiguous notation used by Averyt and Paytan (2003). It has been calculated by these authors from an assumed barium equilibrium content of seawater of 80 nM and from measured values of the Sr contents of barite recovered in sediment cores.

6. Conclusions

- (1) Our calculations show that Sr substitution in barium sulfate does not change the saturation state of the world's ocean with respect to barite and, as such, is not able to provide an explanation for the common presence of barite in a globally undersaturated marine environment.
- (2) The thermodynamic properties of (Ba,Sr)SO₄ solid solution are not definitively established yet, but following the work of Galinier et al. (1989) and of Zhu (2004), there is some evidence that it is regular and continuous. Whatever the solid solution model (ideal or regular/continuous), the calculated saturation indices of the GEOSECS samples do not change much compared to those of pure BaSO₄.

- (3) When a seawater sample is found at equilibrium with a solid solution, the degree of Sr substitution in this solid solution is about 3% for the regular solid solution model.
- (4) Equilibrium values of the Sr mole fraction of (Ba,Sr)-SO₄ solid solutions in the intermediate (0.3–0.8) range are found for seawater samples that are undersaturated. So such solid solutions are not stable in the marine environment. This provides another reason for the bimodal distribution of (Ba,Sr)SO₄ solid solutions in nature, on top of that induced by the large ratio of the end member solubility products.

Acknowledgments

We are greatly indebted to Pierre Glynn, Manuel Prieto and an anonymous reviewer for their helpful suggestions and comments on the manuscript. We also thank Tim Lowenstein for his editorial work.

Associate editor: Tim Lowenstein

References

- Astilleros, J.M., Pina, C.M., Fernandez-Diaz, L., Putnis, A., 2003. Supersaturation functions in binary solid solutions–aqueous solution system. *Geochim. Cosmochim. Acta* **6** (9), 1601–1608.
- Averyt, K.B., Paytan, A., 2003. Empirical partition coefficient for Sr and Ca in marine barite: implications for reconstructing seawater Sr and Ca concentrations. *Geochim. Geophys. Geosys.* **4** (5), 1043. doi:10.1029/2002GC000426.
- Becker, U., Fernandez-Gonzales, A., Prieto, M., Harrison, R., Putnis, A., 2000. Direct calculation of thermodynamic properties of the barite/celestine solid solution from molecular principles. *Phys. Chem. Miner.* **27**, 291–300.
- Bernstein, R.E., Byrne, R.H., Betzer, P.R., Greco, A.M., 1992. Morphologies and transformations of celestine in seawater: the role of acantharians in strontium and barium geochemistry. *Geochim. Cosmochim. Acta* **56** (8), 3273–3279.
- Chan, L.H., Drummond, D., Edmond, J.M., Grant, B., 1977. On the barium data from the Atlantic GEOSECS expedition. *Deep-Sea Res.* **24**, 613–649.
- Church, T.M., Wolgemuth, K., 1972. Marine barite saturation. *Earth Planet. Sci. Lett.* **15**, 35–44.
- Dehairs, F., Lambert, C.E., Chesselet, R., Risler, N., 1987. The biological production of marine suspended barite and the barium cycle in the Western Mediterranean Sea. *Biogeochemistry* **4**, 119–139.
- Felmy, A.R., Rai, D., Moore, D.A., 1993. The solubility of (Ba,Sr)SO₄ precipitates: thermodynamic equilibrium and reaction path analysis. *Geochim. Cosmochim. Acta* **57**, 4345–4363.
- Galini r, C., Dandurand, J.L., Souissi, F., Schott, J., 1989. Sur la caract re non-id al des solutions solides (Ba,Sr)SO₄: Mise en  vidence et d termination des param tres thermodynamiques par des essais de dissolution   25  C.C.R. *Acad. Sci.* **308**, 1363–1368.
- Glynn, P.D., 2000. Solid-solutions solubilities and thermodynamics: sulfates, carbonates and halides. In: Alpers, C.N. Jambor, J.L., Nordstrom, D.K. (Eds.), *Reviews in Mineralogy and Geochemistry Sulfate Minerals: Crystallography, Geochemistry and Environmental Significance*, vol. 40, pp. 481–509.
- Glynn, P.D., Reardon, E.J., 1990. Solid-solutions aqueous–solution equilibria: thermodynamic theory and representation. *Am. J. Sci.* **290**, 164–201.

- Glynn, P.D., Reardon, E.J., Plummer, L.N., Busemberg, E., 1992. Reaction path and equilibrium end-points in solid-solution aqueous-solution systems. *Geochim. Cosmochim. Acta* **54**, 267–282.
- Gooday, A.J., Nott, J.A., 1982. Intracellular barite crystals in two xenophytophores, *Aschemonella ramuliformis* and *Galathea minima* sp. (Protozoa: rhizopoda) with comments on the taxonomy of *A. ramuliformis*. *J. Mar. Biol. Assoc. UK* **62**, 595–605.
- Guggenheim, E.A., 1967. *Thermodynamics*. North-Holland.
- Hanor, J.S., 1969. Barite saturation in sea water. *Geochim. Cosmochim. Acta* **33**, 894–898.
- Hanor, J.S., 2000. Barite-celestine geochemistry and environments of formation. In: Alpers, C.N., Jambor, J.L., Nordstrom, D.K. (Eds.), *Reviews in Mineralogy and Geochemistry* vol. 40, *Sulfate Minerals: Crystallography, Geochemistry and environmental significance*, pp. 193–275.
- Jacquet, S.H.M., Dehairs, F., Rintoul, S., 2004. A high resolution transect of dissolved barium in the Southern Ocean. *Geophys. Res. Lett.* **31**, 14301–14305.
- Jeandel, C., Dupre, B., Lebaron, G., Monnin, C., Minster, J.-F., 1996. Longitudinal distributions of dissolved barium, silica and alkalinity in the western and southern Indian Ocean. *Deep-Sea Res. Part I* **4** (1), 1–31.
- Konigsberger, E., Gamsjager, H., 1992. Comment on “solid solution–aqueous solution equilibria: thermodynamic theory and representation” by Glynn P.D. and Reardon E. *J. Am. J. Sci.* **292**, 199–214.
- Kotel'nikov, A.R., Kabalov, Y.K., Zezyulya, T.N., Mel'chakova, L.V., Ogorodova, L.P., 2000. Experimental study of celestine–barite solid solution. *Geochem. Int.* **3** (12), 1181–1187.
- Lippmann, F., 1977. The solubility products of complex minerals, mixed crystals and three-layer clay minerals. *Neues Jb. Miner. Abh.* **130**, 243–263.
- Lippmann, F., 1980. Phase diagrams depicting aqueous solubility of binary mineral system. *Neues Jahrb Mineral Abh.* **139**, 1–25.
- Lippmann, F., 1982. Stable and metastable solubility diagrams for the system $\text{CaCO}_3\text{--MgCO}_3\text{--H}_2\text{O}$ at ordinary temperature. *Bull. Mineral.* **105**, 273–279.
- Monnin, C., 1999. A thermodynamic model for the solubility of barite and celestine in electrolyte solutions and seawater to 200 °C and to 1 kbar. *Chem. Geol.* **153**, 187–209.
- Monnin, C., Jeandel, C., Cattaldo, T., Dehairs, F., 1999. The marine barite saturation state of the world's oceans. *Mar. Chem.* **65** (3–4), 253–261.
- Ostlund, H., Craig, H., Broecker, W., Spencer, D. 1987. *Geosecs Atlantic, Pacific and Indians Ocean Expeditions. Shorebased Data and Graphics*. NSF.
- Pitzer, K.S., Brewer, L., 1961. *Thermodynamics*. McGraw-Hill, NY.
- Plummer, N.L., 1992. Geochemical modeling of water–rock interaction: past, present, future. *Water-Rock interaction*, 23–33.
- Prieto, A., Putnis, A., Fernandez-Diaz, L., 1993. Crystallization of solid solutions from aqueous solutions in a porous medium: zoning in $(\text{Ba,Sr})\text{SO}_4$. *Geol. Mag.* **130** (3), 289–299.
- Prieto, M., Fernandez-Gonzalez, A., Putnis, A., Fernandez-Diaz, L., 1997. Nucleation, growth, and zoning phenomena in crystallizing $(\text{Ba,Sr})\text{CO}_3$, $\text{Ba}(\text{SO}_4\cdot\text{CrO}_4)$, $(\text{Ba,Sr})\text{SO}_4$, and $(\text{Cd,Ca})\text{CO}_3$ solid solutions from aqueous solutions. *Geochim. Cosmochim. Acta* **61** (16), 3383–3397.
- Prieto, M., Fernandez-Gonzales, A., Becker, U., Putnis, A., 2000. Computing Lippmann diagram from direct calculation of mixing properties of solid solutions: application to the barite–celestite system. *Aquat. Geochem.* **6**, 133–146.
- Prigogine, I., Kondepudi, D., 1999. *Thermodynamique. Des moteurs thermiques aux structures dissipatives*. Odile Jacob, Paris.
- Putnis, A., Junta-Rosso, J.L., Hochella, M.F., 1995. Dissolution of barite by a chelating agent: an atomic force microscopy study. *Geochim. Cosmochim. Acta* **59** (22), 4623–4632.
- Rushdi, A.I., McManus, J., Collier, R.W., 2000. Marine barite and celestine saturation in seawater. *Mar. Chem.* **69**, 19–31.
- Sternberg, E., Tang, D., Ho, T.-Y., Jeandel, C., Morel, F.M.M., 2005. Barium uptake and adsorption in diatoms. *Geochim. Cosmochim. Acta* **69** (11), 2745–2752.
- Tekin, E., Varol, B., Sayili, I.S., Elerman, Y., 2002. Indications of intermediate compositions in the $\text{BaSO}_4\text{--SrSO}_4$ solid-solution series from the Bahceciktepe celestine deposit, Sivas, East-Central Anatolia, Turkey. *Can. Mineral.* **40**, 895–908.
- Van Beek, P., Reyss, J.-L., Bonte, P., Schmidt, S., 2003. Sr/Ba in barite: a proxy of barite preservation in marine sediments? *Mar. Geol.* **199** (3–4), 205–220.
- Zhu, C., 2004. Coprecipitation in the barite isostructural family: 1. binary mixing properties. *Geochim. Cosmochim. Acta* **68** (16), 3327–3337.